Supporting Information

High Performance P(VDF-TrFE) Nanogenerator with Self-Connected and Vertically Integrated fibers by Patterned EHD Pulling

Xiaoliang Chen,† Hongmiao Tian,† Xiangming Li,† Yaopei Zhou,† Jinyou Shao,† Yucheng Ding,†* and Ningli An§*

†Micro- and Nano-technology Research Center, State Key Laboratory for Manufacturing Systems Engineering, Xi'an Jiaotong University, Xi'an, Shaanxi 710049, China

§College of Printing and Packaging Engineering, Xi'an University of Technology, Xi'an, Shaanxi 710048, China

*Corresponding author: jyshao@mail.xjtu.edu.cn(Jinyou Shao);

S1. Dynamic deformation numerically simulated for the pre-formed polymer affected by an electric potential

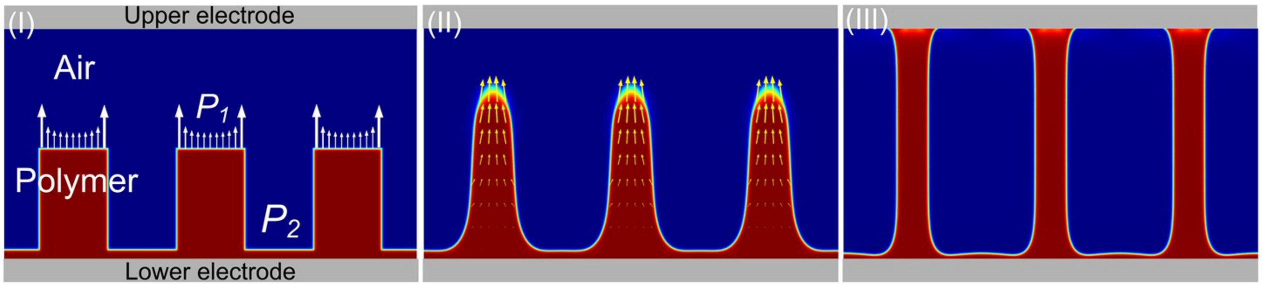

Figure S1. Dynamic deformation numerically simulated for the pre-formed polymer affected by an electric potential at the beginning (I), middle (II) and ending (III) of the EHD process, with the white arrows the vectored Maxwell force on the polymer surface, and the yellow arrows representing the vectored flowing velocity

The EHD behavior of the dynamic deformation can be explained by a proportional relationship between the electric field E_p and the electrostatic force (or Maxwell force) P_e on the air-polymer interface and , as expressed in the following:[1]

$$P_e = \frac{1}{2}\varepsilon_0\varepsilon_p(\varepsilon_p - 1)E_p^2 \quad (1)$$

where ε_0 is the dielectric permittivity of the vacuum, ε_p the relative dielectric permittivity of the polymer. Obviously, the non-uniform electric field on the air-polymer interface spatially modulated by the pre-formed micropillar array between the electrode pair will have a maximum intensity at each micropillar top. Such a distributed electric field produces a difference of the Maxwell force at the polymer protrusion, P_1, and the one at the polymer valley, P_2 (with too small a magnitude to be visible in a vectored vector mapping), as shown in Figure S1. With a proper voltage, the differential Maxwell force becomes large enough to pull the micropillars upward by overcoming the surface tension and viscous resistance. The upward moving of the micropillars induces an increasing spatial fluctuation in the electric field or Maxwell pressure, which in turn pulls the micropillars upward further. It is this mutually positive feedback effect that extends the micropillars progressively into a final contact with the upper electrode.[2, 3] It can be seen that velocity within the micropillars is dominantly vertical during the EHD process, practically leading to a fully axial elongation which is quite desirable for an anisotropic alignment of the dipoles in the P(VDF-TrFE) microfibers.

S2. Switching test conducted by reversing the electrode connections

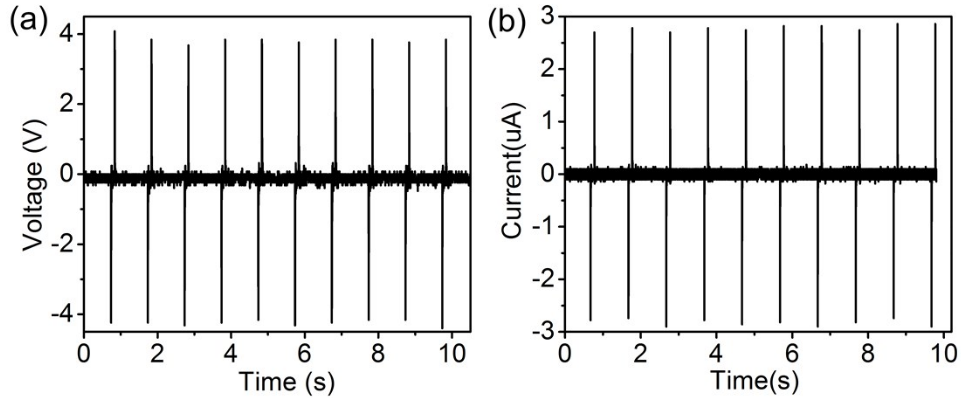

Figure S2. Switching of the output voltage (a) and current (b) on reversing the electrode connections. For polarity connectivity, the SCVIG generates positive peaks in the pressing state. To the contrary, for a reversed connectivity, the negative peaks are generated in the pressing state instead, demonstrating that the output signal is indeed from the piezoelectric microfiber.

S3. Optical image of two SCVIG devices placed together for a superposition test

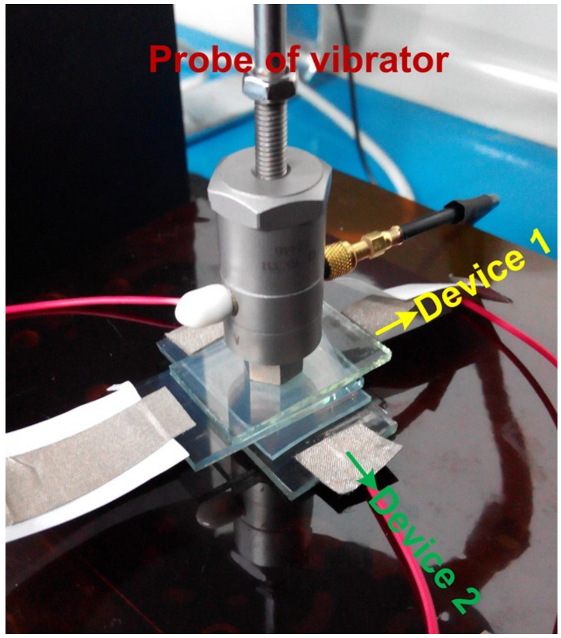

Figure S3. Optical image of two SCVIG devices placed together for a superposition test. It is also known to be a way to rule out any artificial noise caused by other effects.

S4. The piezoelectric comparison of P(VDF-TrFE) and PMMA microfiber array

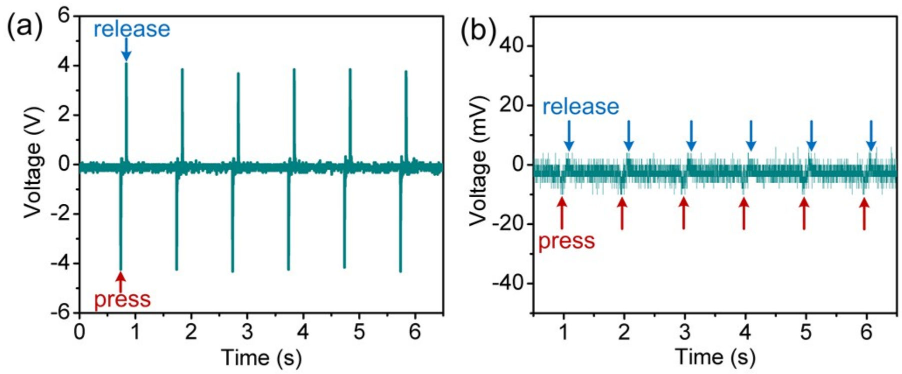

Figure S4. Voltage output of a P(VDF-TrFE) microfiber array (a), and of PMMA microfiber array (b), subject to a periodic press-and- release excitation, which proves that the output from the SCVIG is purely due to the piezoelectricity.

S5. The detailed simulation process conducted using the COMSOL software package

A standard physical model for piezoelectric simulation as commonly used by previous researchers is adopted in this study.[4,5] In our simulation, all the calculated unit blocks were modeled as 20μm×20μm which reflect actual dimensions of the fabricated device. Figure S5-1a shows the geometrical configuration of the finite element method (FEM) simulation model. The lower electrode was fixed and the bottom of the P(VDF-TrFE) fiber was electrically grounded. After the structural setup, a constant pressure was applied to the upper electrode of the device. Figure S5-1b shows the three unit models after meshing. The unit (I) has a diameter of 6μm and a height of 50μm. The unit (II) has a diameter of 10μm and a height of 30μm. The unit (III) represents a flat film unit with a height of 50μm.

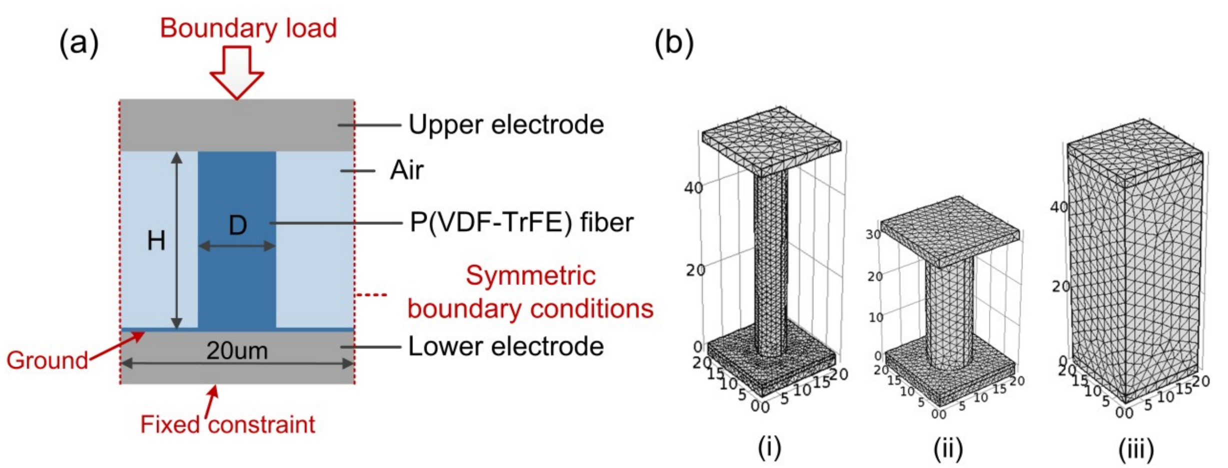

Figure S5-1. (a) The geometrical configuration of the FEM simulation model. (b) The three unit models after meshing.

Materials used:

Property	Variable	Expression	Unit
Elasticity matrix	C_E	$\begin{bmatrix} 3.613e9 & 1.6135e9 & 1.4210e9 & 0 & 0 & 0 \\ 1.6135e9 & 3.1312e9 & 1.3106e9 & 0 & 0 & 0 \\ 1.4210e9 & 1.3106e9 & 1.6303e9 & 0 & 0 & 0 \\ 0 & 0 & 0 & 0.5501e9 & 0 & 0 \\ 0 & 0 & 0 & 0 & 0.5900e9 & 0 \\ 0 & 0 & 0 & 0 & 0 & 0.6901e9 \end{bmatrix}$	Pa
Coupling matrix	e	$\begin{bmatrix} 0 & 0 & 0 & 0 & -0.0159 & 0 \\ 0 & 0 & 0 & -0.0127 & 0 & 0 \\ 0.0321 & -0.0040 & -0.0212 & 0 & 0 & 0 \end{bmatrix}$	C/m^2
Density	ρ	1780	kg/m^3
Relative permittivity	ε_r	18	1

Other parameters except the geometrical shape are kept the same for the comparison as fair as possible. An identical external load (50kPa) was applied to the upper electrode of the three units. After the elastic, electric and piezoelectric equations were solved,[6] the potential profile can be extracted.

Poisson equations:

$$-\nabla \cdot T = F_V$$

$$-\nabla \cdot D = \rho_V$$

Piezoelectric equations:

$$T = C_E \cdot S - e^T \cdot E$$

$$D = e \cdot S + \varepsilon \cdot E$$

Where: F=force, ρ =density, T=stress,

S=strain, E=electric field, D= electric displacement,

ε =Permittivity, C_E= Elasticity matrix, e= Coupling matrix

Figure S5-2 shows the 3-D surface plot of simulated peak piezoelectric potential of three unit blocks. Because PVDF has a negative piezoelectric coefficient along the axial direction, the top surface exhibits a positive potential compared to the ground potential at the bottom. The unit microfiber (i) device has a diameter of 6μm and a height of 50μm, the potential is in the range from 0 to 5.2871V. The unit microfiber (ii) device has a diameter of 10μm and a height of 30μm, and the potential varies from 0 to 1.561V. The unit (iii) represents a flat film unit with a height of 50μm, and the peak piezoelectric potential has a minimum value 0.5042V.

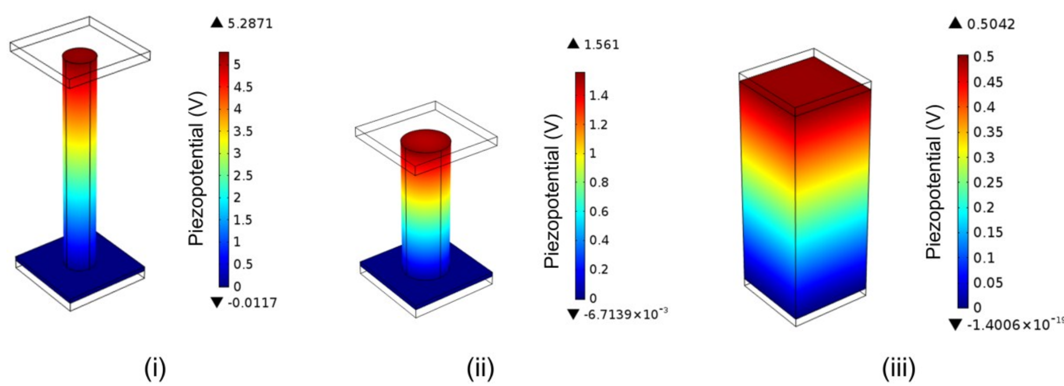

Figure S5-2. 3-D surface plot of simulated peak piezoelectric potential of three unit blocks.

S6. Calculation of the voltage drop across the SCVIG device

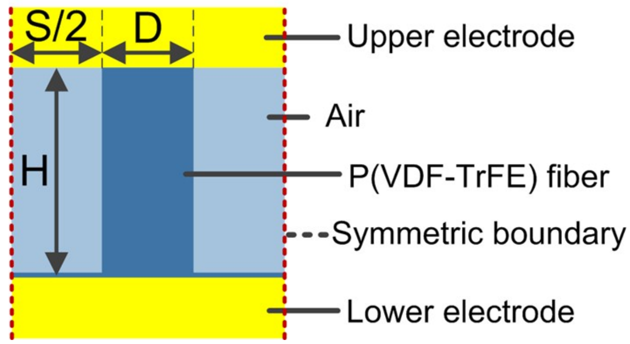

Figure S6. Schematic diagram of a calculated P(VDF-TrFE) microfiber unit

Figure S6 shows the schematic diagram of a calculated unit which a microfiber is sandwiched between two electrodes. The voltage drop across the unit can be calculated by the ratio of total charge collected at the electrodes over the total capacitance:

$$V = \frac{Q}{C} \qquad (1)$$

Where Q is the total charge collected at the electrodes corresponds to the charge generated by the microfiber, C is the total capacitance which is the sum of the capacitance of the microfiber and the air gap.

The charge generated by the microfiber is:

$$Q = Q_f = C_f \cdot V_f = \frac{\varepsilon \cdot \pi D^2/4}{H} \cdot V_f \qquad (2)$$

where ε is permittivity of P(VDF-TrFE), D is the diameter of the microfiber, H is the height of the microfiber and V_f is the piezopotential across the microfiber.

The total capacitance is:

$$C = C_f + C_a \qquad (3)$$

in which the air capacitance is:

$$C_a = \varepsilon_0 \cdot \frac{A - A_f}{H} = \varepsilon_0 \cdot \frac{(\mathrm{S}+\mathrm{D})^2 - \pi D^2/4}{H} \qquad (4)$$

Where ε_0 is permittivity of the air, S is the gap between fibers.

Combination of Eqs. (1)-(4) gives the voltage drop across one P(VDF-TrFE) microfiber unit as:

$$V = \frac{V_f \cdot \varepsilon_r}{\frac{4}{\pi} \cdot \left(\frac{S+D}{D}\right)^2 + \varepsilon_r - 1} \qquad (5)$$

where ε_r is the relative permittivity of P(VDF-TrFE), ε_r =18

In the case of Microfiber (I), V_f =5.2871V, D=6μm, S=14μm, the calculated $V_{Microfiber(I)}$=3.055V

In the case of Microfiber (II), V_f=1.561V, D=10μm, S=10μm, the calculated $V_{Microfiber(II)}$=1.272V

S7. The output voltage measured used to drive the LCD screen

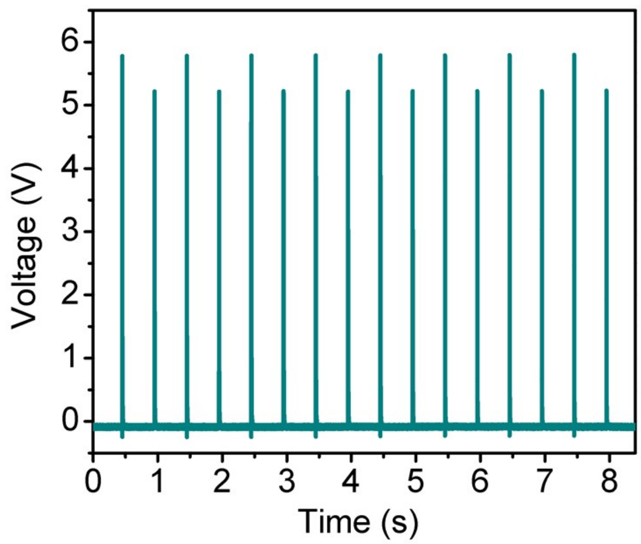

Figure S7. The output voltage measured from the SCVIG device at an impact frequency of 1 Hz, which was used to drive the LCD screen.

References:

[1] J. Zeng, T. Korsmeyer, Lab on a Chip. 2004, 4, 265.

[2] H. Tian, Y. Ding, J. Shao, X. Li, H. Liu, Soft Matter. 2013, 9, 8033.

[3] P. Goldberg ‐ Oppenheimer, P. Kohn, R. M. Langford, U. Steiner, Small. 2012, 8, 2595.

[4] Y. Wang, L. Wang, T. Yang, X. Li, X. Zang, M. Zhu, K. Wang, D. Wu, H. Zhu, *Advanced Functional Materials* **2014**, *24*, 4666.

[5] M.-L. Seol, H. Im, D.-I. Moon, J.-H. Woo, D. Kim, S.-J. Choi, Y.-K. Choi, *ACS nano* **2013**, *7*, 10773.

[6] K. Lefki, G. Dormans, *Journal of applied physics* **1994**, 76, 1764.

Supplementary video

Video S1. The SCVIG was driven by a slight pressing motion of finger tapping, and showed a perfect synchronization of the finger motion with induced voltage.

Video S2. Commercial RGBY LEDs lit up by the power generated from a SCVIG device.

Video S3. A Seven-segment indicator was powered up using the charged electricity in capacitor.

Video S4. A LCD screen directly driven by a SCVIG device.